

# Fiber Optic Sensors for Noncontact Process Monitoring in a Microwave Environment

B. Degamber, G. F. Fernando

Engineering Systems Department, Cranfield University, Royal Military College of Science, Shrivenham, Swindon, SN6 8LA, United Kingdom

Received 9 July 2002; accepted 6 January 2003

**ABSTRACT:** This article reports on the design and development of two fiber optic sensing systems that facilitate the cure monitoring of an epoxy/amine thermoset in a microwave oven. First, the design, construction, and evaluation of a fiber optic probe were necessary so that noncontact diffuse reflectance spectra could be obtained during the curing of the resin in a microwave oven. Second, a low-cost, disposable fiber optic temperature sensor had to be developed for

use in the microwave oven because the use of conventional metal-based thermocouples was not possible. The deployment of the two sensor systems was demonstrated successfully. © 2003 Wiley Periodicals, Inc. *J Appl Polym Sci* 89: 3868–3873, 2003

**Key words:** curing of polymers; FT-IR; sensors; fibers

## INTRODUCTION

The cure monitoring of advanced fiber-reinforced composites continues to attract significant global attention, with productivity and product quality issues being the predominant drivers. For example, the economic benefits include (1) turning off the power to the processing equipment once the desired level of cure has been achieved and (2) controlling the processing parameters (the rate of heating, isothermal hold period, pressure, and vacuum) to optimize or compensate for the chemical state of the resin or the thickness of the composite being processed. In terms of product quality, the use of sensor systems to infer the compliance with specifications will accrue commercial advantages. Furthermore, the deployment of the same sensor system to infer structural integrity or health monitoring has obvious attractions.

With respect to the processing of composites, the thermal energy required for initiating the cure reaction has traditionally been achieved through conduction, radiation, and convection-type heating arrangements in the processing equipment. However, in recent years, there has been a resurgence in interest in alternative heating methods.<sup>1</sup> Electromagnetic heating

has generated significant interest because it has the potential to offer faster curing times and improved curing efficiency.<sup>2,3</sup> Ultraviolet radiation suffers from the fact that it has a limited penetration depth and so cannot be used to process thick components. X-rays provide a very low dose rate, which results in an extremely long curing time.  $\gamma$  radiation, although permitting deeper penetration, is not generally used because the radiation has a long half-life, which can have safety implications. Electron-beam accelerators operating in the megaelectronvolt region offer high penetration depths and the prospect of fast curing.<sup>4</sup> However, the relative cost associated with high-voltage accelerators is prohibitive for the routine processing of composites. In terms of the costs and facilities needed to use conventional composite processing procedures (simultaneous vacuum bagging and pressure), microwave curing has proven to be effective.<sup>5</sup>

Microwave processing has several advantages; for example, there is a decrease in the processing time and the energy usage.<sup>6</sup> If the electric field is assumed to be uniform throughout the volume of a sample interacting with a microwave field, the power absorbed per unit volume by the material is given by<sup>7</sup>

$$P = 2\pi\epsilon_0 f \epsilon'' E^2 \quad (1)$$

where  $P$  is the power dissipated ( $\text{Wm}^{-3}$ ),  $K$  (equal to  $2\pi\epsilon_0$ ) is a constant ( $55.61 \times 10^{-12} \text{ Fm}^{-1}$ ),  $f$  is the applied frequency (Hz),  $E$  is the electric field ( $\text{Vm}^{-1}$ ),  $\epsilon''$  (equal to  $\epsilon' \tan \delta$ ) is the dielectric loss factor,  $\epsilon'$  is the real part of the relative dielectric constant, and  $\tan \delta$  is the loss tangent.  $\epsilon''$  is influenced by the sample temperature and applied frequency.

Correspondence to: G. F. Fernando (g.f.fernando@rmcs.cranfield.ac.uk).

Contract grant sponsor: Engineering and Physical Sciences Research Council.

Contract grant sponsor: Engineering Systems Department at Cranfield University.

Contract grant sponsor: Engineering and Aerospace Club.

With respect to the microwave processing of materials, monitoring the temperature in the vicinity of the specimen is a vital requirement for facilitating effective process control. This poses a problem for microwave processing because conventional, low-cost metallic thermocouples cannot be used inside the ovens or cavities. However, with the proliferation of fiber optic sensors, a number of efficient temperature-measuring devices have become commercially available. The majority of the fluoroptic sensors are based on the decay of fluorescence with time<sup>8</sup> and on infrared radiation thermometers.<sup>9</sup> The cost associated with each fiber optic sensor is relatively high, and for most end-use applications, using these sensors as disposable devices is not a viable economic option.

In the context of cure monitoring, a number of techniques based on fiber optics have successfully been demonstrated.<sup>10</sup> These include (1) evanescent spectroscopy,<sup>11</sup> (2) attenuated total reflection spectroscopy,<sup>12</sup> (3) transmission spectroscopy with a modified extrinsic Fabry–Perot interferometry (EFPI) capillary,<sup>13</sup> and (4) noncontact reflectance spectroscopy.<sup>14</sup> All these have been conducted in the infrared region of the electromagnetic spectrum. Fiber optic Raman spectroscopy has also been used for cure monitoring.<sup>15</sup>

This article reports on the design, development, and evaluation of (1) a noncontact fiber optic probe that facilitates cure monitoring and (2) a low-cost fiber optic temperature sensor for deployment in a microwave oven.

## EXPERIMENTAL

### Noncontact fiber optic probe

The fiber optic probe consisted of a bifurcated bundle of silica–silica low-OH<sup>-</sup> 200/220- $\mu\text{m}$  fibers supplied by BFI Optillas, Ltd. The probe end of the bifurcated fiber optic bundle consisted of a random arrangement of optical fibers. These were potted in a silicone elastomer (Silguard 184) from Dow Corning (South Glamorgan, UK). The light input and detector ends of the bifurcated bundle were potted in two sub-miniature A type (SMA) connectors. The ends of the bifurcated bundle were polished with conventional procedures for the maximum transmission and reception of the light.

### Infrared spectroscopy

The light input and output ends of the fiber probe were connected to a Nicolet Nexus Fourier transform infrared spectrometer (Cambridge, UK), which was set to operate in the near-infrared range between 4000 and 11000  $\text{cm}^{-1}$ . The probe end of the bifurcated bundle was located 1 mm above the resin inside a

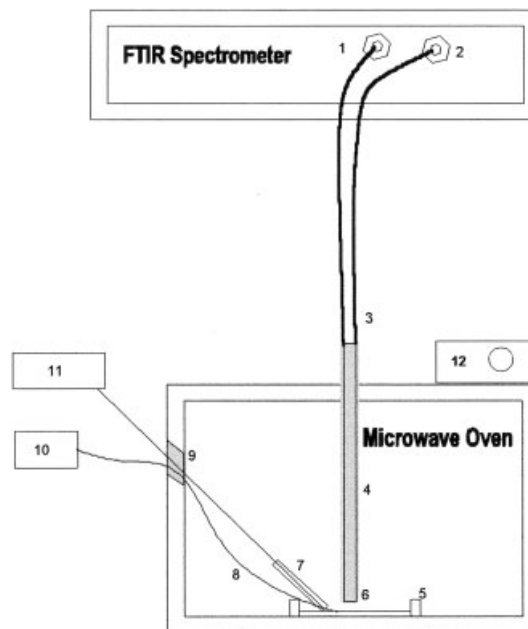


**Figure 1** Schematic illustration of the experimental setup for cure and temperature monitoring inside the modified microwave oven with fiber optic probes (see the text for details).

modified microwave oven. Spectra were collected at a resolution of 8  $\text{cm}^{-1}$  (24 scans).

### Microwave oven

A Sanyo EM-P1010 microwave oven (Gamma Consultants Ltd., Kent, UK) was custom-modified to accommodate the fiber optic probe, which was to be located at 0 or 45° to the base at which the test specimen was located (see Fig. 1). The oven was fitted with a voltage controller to facilitate the processing power (to be specified). In this study, the curing was carried out at four different power levels: 400, 500, 600, and 700 W.

The various components shown in Figure 1 are as follows: (1,2) the ports on the Fourier transform infrared spectrometer used for launching the light into (3) the bifurcated noncontact probe and for detecting the reflected light off the test specimen, (4) a glass capillary used to locate and protect the fiber optic probe inside the microwave oven, (5) the glass fixture used to contain the resin system, (6) the active end of the fiber optic probe containing the optical fibers, (7) a capillary tube sealed at one end (to keep the resin out) and containing the commercially available temperature fiber optic probe, (8) the custom-made disposable EFPI sensor, (9) an orifice in the side of the microwave oven inclined at 45° and used to accommodate the reflectance probe at this angle in relation to the surface of the test specimen, (10,11) the charge coupled device (CCD) spectrometer and Fiso instrumentation, and

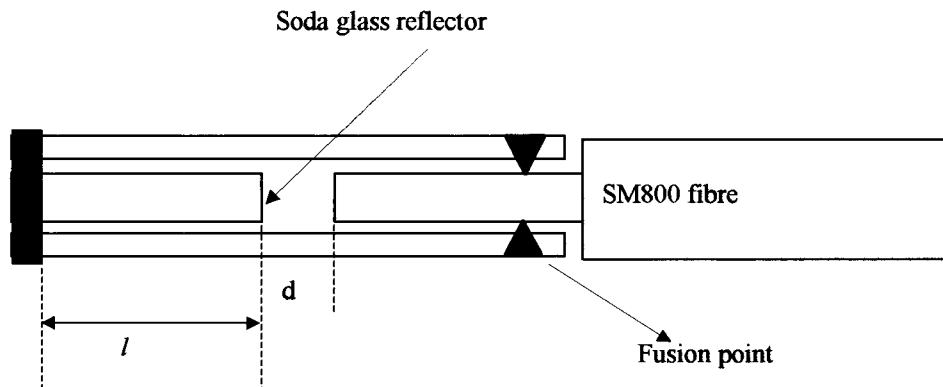


Figure 2 Schematic illustration of the fiber optic EFPI temperature sensor design.

(12) the variable power controller for the microwave oven.

### Fiber optic temperature sensor

The temperature sensor developed in this study was based on EFPI. The interference of two or more light beams occurs when light reflecting off two mirrors placed in close proximity to each other are superimposed. The interference pattern varies with the distance between the two reflecting plates. When a monochromator is used as the light source, the absolute cavity (gap) length ( $d$ ) of the EFPI sensor can be measured from the wavelength separation in the scanning of one complete interference fringe.<sup>16</sup>

$$d = \frac{\lambda_2 \lambda_1}{2(\lambda_1 - \lambda_2)} \quad (2)$$

The sensor was made of a precision-cleaved SM800 silica fiber (Fibercore Ltd., Southampton, UK) and a cleaved soda glass rod with the end faces being placed in close proximity (usually between 60 and 100  $\mu\text{m}$ ) and secured in a precision-bore silica glass capillary via two fusion joints (see Fig. 2). Approximately 4% of the light was reflected back from the cleaved ends, and the interference created was detected with an Ocean Optics S2000 CCD spectrometer (Duiven, The Netherlands).

When the sensor was subjected to a temperature rise, the greater expansion of the soda glass ( $9.5 \times 10^{-6}$  vs  $0.5 \times 10^{-6} \text{ } ^\circ\text{C}^{-1}$  for silica) caused the gap between its end face and that of the fiber to decrease. Therefore, the rise in the temperature caused a linear decrease in the cavity or gap length, and the variation in the air gap ( $\nabla d$ ) with the temperature is given by

$$\nabla d = [l(\alpha_{\text{So}} - \alpha_{\text{Si}})]\nabla T \mu\text{m} \quad (3)$$

where  $\alpha_{\text{So}}$  and  $\alpha_{\text{Si}}$  are the expansion coefficients of the soda glass rod and the capillary, respectively;  $\nabla T$  is

the temperature change; and  $l$  is the length of the free-moving soda glass rod.

The sensor was evaluated in a tubular furnace that was instrumented with an Eurotherm temperature controller (Worthing, UK) and calibrated against a K-type thermocouple. Interference spectra from EFPI were recorded with the CCD spectrometer with a resolution of 0.14 nm and powered by a superluminescent diode (SLD) light source with a center wavelength at 850 nm.

The performance of EFPI in the microwave oven was compared against a commercially available fiber optic temperature sensor from Fiso Technology (Quebec, Canada). The Fiso temperature probe (FOT-L) had a maximum operating temperature of 250 $^\circ\text{C}$ , and it was connected to a UMI four-channel signal conditioner.

### Resin system

The resin used was a commercially available (Vantico, Cambridge, UK) epoxy [LY3505 (diglycidyl ether of bisphenol A/F)], with an amine [XB3403 (propylene diamine)] as a hardener. These components were mixed in a stoichiometric ratio of 100:35. The cure schedule recommended by the manufacturer was 6 h at 80 $^\circ\text{C}$ .

## RESULTS AND DISCUSSION

### Noncontact cure monitoring probe

The noncontact reflectance spectra of the epoxy/amine resin as a function of microwave processing at 500 W is presented in Figure 3. The spectrum at the start of the cure shows the epoxy stretching and bending vibration band at 4530  $\text{cm}^{-1}$ . This absorption band has been used previously for monitoring the extent of cure.<sup>17</sup> In this work, the amine overtone of the symmetric and asymmetric stretch at 6526  $\text{cm}^{-1}$  was used in conjunction with the reference (unreacting) CH

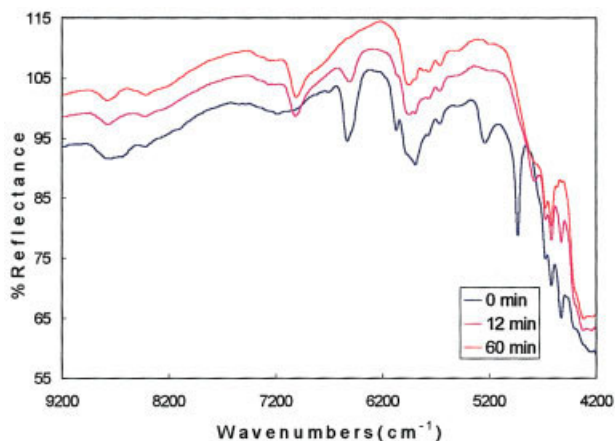


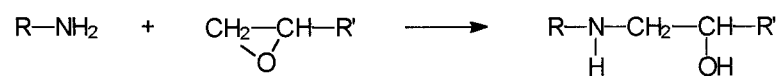
**Figure 3** Near-infrared spectra of the epoxy/amine resin system recorded with a reflectance probe at the beginning of the cure and after 40 min of the cure inside the microwave oven at 500 W. [Color figure can be viewed in the online issue, which is available at [www.interscience.wiley.com](http://www.interscience.wiley.com).]

stretching peak at  $4619\text{ cm}^{-1}$  for calculating the depletion of the amine as a function of the processing time. The formation of the hydroxyl peak at  $7000\text{ cm}^{-1}$  is clearly visible in the spectra obtained after 12 and 60 min of cure at 500 W. This agrees with the generalized reaction scheme illustrated in Figure 4, in which the primary amine (hardener) is shown to react with the epoxy resin with the formation of hydroxyl and secondary amine functional groups. The secondary amine is then capable of reacting with another epoxy group, eventually leading to the formation of a highly crosslinked structure.

In a comparison of the spectra shown in Figure 4, a shift is apparent in the relative position of the baseline after 12 and 60 min of the cure reaction. The shift in the baseline may be due to one or more of the following factors:

1. The expansion of the microwave chamber during heating.

#### Primary amine-epoxy addition



#### Secondary amine-epoxy addition

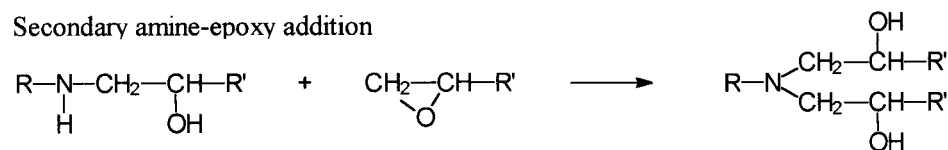


**Figure 4** Generalized reaction scheme illustrating the reaction between the hardener (amine) and the epoxy resin. The scheme illustrates the depletion of the amine and epoxy groups along with the formation of hydroxy ( $\text{—OH}$ ) functional groups.

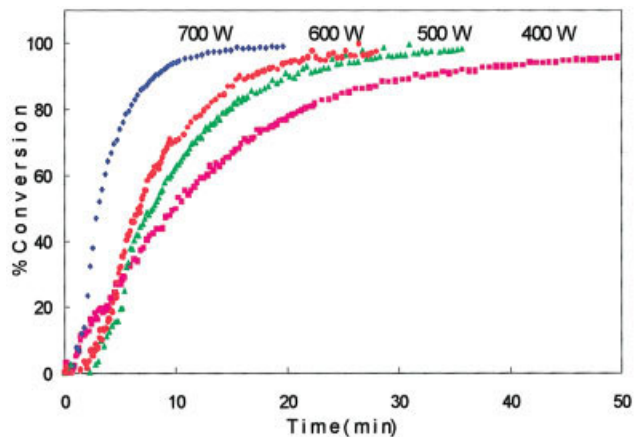


**Figure 5** Extent of cure at four different power levels with the microwave oven. [Color figure can be viewed in the online issue, which is available at [www.interscience.wiley.com](http://www.interscience.wiley.com).]

2. The vibration of the magnetron as the material is heated. This may cause the fiber optic probe to vibrate in a random fashion.
3. The expansion of the probe and substrate during heating.
4. The resin shrinkage during cure.
5. The lowering of the refractive index of the fiber optic probe during heating.
6. The increase in the refractive index of the resin as it cures.

Further studies are being carried out to isolate these factors so that we can obtain a better understanding of the reasons for the observed variation in the baseline as the cure proceeds.

The data presented in Figure 3 were analyzed in terms of the extent of cure, and they are presented in Figure 5 along with the results for the other microwave power levels used in this study. The temperature was also noted during the cure reaction with a commercial sensor from Fiso Technology. Note that

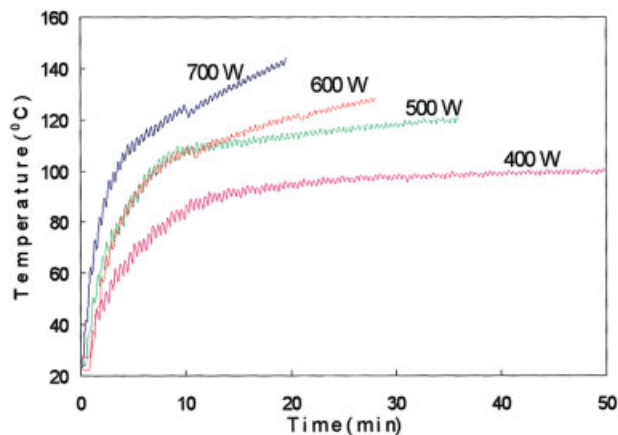


**Figure 6** Temperature profile inside the microwave oven at four power levels. [Color figure can be viewed in the online issue, which is available at [www.interscience.wiley.com](http://www.interscience.wiley.com).]

this sensor was placed in close proximity to the resin, but not in direct contact with it. The following equation was used to calculate the extent of cure ( $\alpha$ ):

$$\alpha = 1 - [(A_{NH})/(A_{CH})]_t / [(A_{NH})/(A_{CH})]_0 \quad (4)$$

where  $(A_{NH}/A_{CH})_t$  and  $(A_{NH}/A_{CH})_0$  represent the ratios of the area of NH to the reference CH peaks after time  $t$  and 0 min, respectively.

The graph shows that for the 700-W power level, full cure was achieved in just under 20 min, whereas in all the other cases, the percentage cure was about 98–99%. The time to an 80% cure was 20 min at 400 W, 15 min at 50 W, 12 min at 600 W, and 7 min at 700 W.

The corresponding temperature curves for this data set are shown in Figure 6. At 400 W, an isothermal condition is achieved, under which the temperature stabilizes around 100°C after 20 min. The 600- and 700-W data sets show a small discontinuity in the temperature at 10-min intervals. This is due to the fact that above a power setting of 500 W, the microwave oven has an in-built safety feature that cuts the power off after 10 min of continuous use. This meant that the power had to be switched on again manually, and this resulted in a small decrease in the measured temperature. The temperature–time trace in Figure 6 exhibits a periodic oscillation. This can be attributed to the mode of operation of the microwave oven, in which the power to the magnetron is modulated to ensure uniform heat distribution.

#### Fiber optic temperature sensor performance

The temperature in the previous section was recorded with the Fiso sensor placed in close proximity to the curing resin. This may not necessarily reflect the true temperature inside the resin or at the point at which the reflectance spectra are taken.<sup>18</sup> To address this problem,

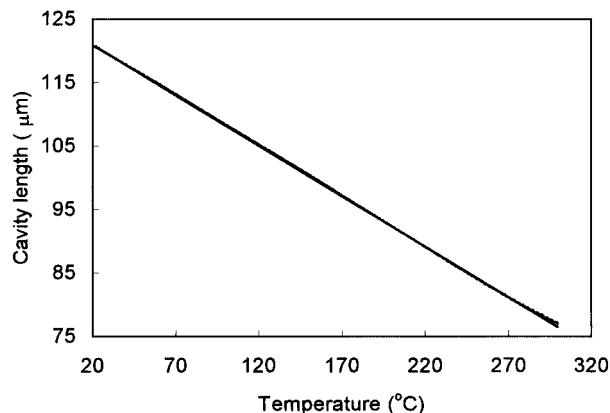


**Figure 7** Response of the EFPI temperature sensor from the ambient temperature to 300°C inside the tubular furnace.

we evaluated the disposable fiber optic sensor described previously. Figure 7 presents the response of the EFPI sensor from the ambient temperature to 300°C, at which point a repeatable linear response was obtained. The accuracy of the sensor was  $\pm 0.5^\circ\text{C}$ . This was dictated by the resolution of the CCD spectrometer, which was 0.14 nm. The accuracy could be increased to  $\pm 0.1^\circ\text{C}$  or better with a higher resolution spectrometer.

Another sensor with the same configuration, but with an initial cavity length of 94  $\mu\text{m}$ , was tested inside a microwave oven from the ambient temperature to 120°C. The power was increased in steps of 100 W from 400 W to 1 kW to increase the temperature inside the microwave oven. This progressive stepwise increase in the power level was necessary, as the temperature inside the microwave oven tended to stabilize with time. The response is shown in Figure 8, and the accuracy was calculated to be less than  $\pm 1^\circ\text{C}$ . The noisy response was attributed to the vibration of the magnetron inside the microwave oven during the heating cycle and the manual power increment that was necessary for the desired temperature to be achieved.

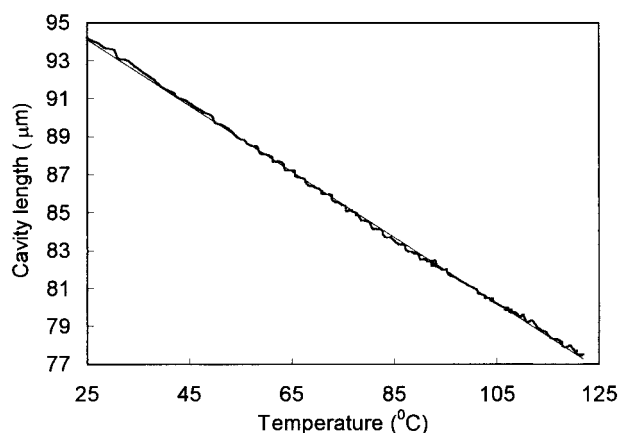


**Figure 8** Response of the EFPI temperature sensor inside the microwave oven as a function of temperature.

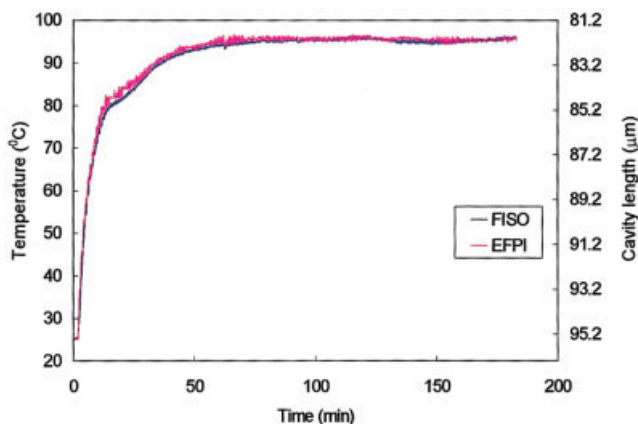


**Figure 9** Response of the modified EFPI sensor during the curing of the epoxy resin system. [Color figure can be viewed in the online issue, which is available at [www.interscience.wiley.com](http://www.interscience.wiley.com).]

The custom-modified EFPI sensor was also tested inside the microwave oven while the resin system was being cured at a power level of 400 W. The temperature was also monitored with the commercially available Fiso sensor. The response of the two sensors is shown in Figure 9. There was an excellent correlation between the two sensors, showing that the in-house-built low-cost sensor could be used to monitor the temperature *in situ* during the cure inside the microwave oven.

## CONCLUSIONS

This study demonstrated the successful deployment of two optical fiber sensors inside a microwave oven for monitoring the cure and temperature *in situ* during a curing process. The cure experiments were conducted at four different power levels, and in each case, spectra were collected, with the result that the extent of cure was obtained in real time. The tools developed here will facilitate the simulation of temperature profiles in a microwave oven being reproduced in a conventional oven or a differential scanning calorimeter. This will

enable the relative cure mechanisms of the different methods of heating to be compared. Finally, it will also help to elucidate whether microwave processing is significantly different from conventional thermal curing.

The assistance given by R. Day, B. Ralph, T. Liu, C. Doyle, C. Tuck, and Lumen Photonics is duly acknowledged.

## References

- Mijovic, J.; Wijaya, J. *Macromolecules* 1990, 23, 3761.
- Chia, H. L.; Jacob, J.; Boey, F. Y. C. *J Polym Sci Part A: Polym Chem* 1996, 34, 2087.
- Boey, F. Y. C.; Lee, T. H. *Radiat Phys Chem* 1991, 38, 419.
- Nablo, S. V. *J Ind Irradiat Technol* 1985, 3, 41.
- Boey, F. Y. C.; Rath, S. K. *Adv Polym Technol* 2000, 19, 194.
- Freeman, G. *J Microwave Power* 1972, 7, 353.
- Thostenson, E. T.; Chou, T. W. *Compos A* 1999, 30, 1055.
- Grattan, K. T. V.; Zhang, Z. Y. *Fibre Optic Fluorescence Thermometry*; Chapman & Hall: New York, 1995.
- Yarlagadda, P. K. D. V.; Choek, E. C. *J Mater Process Technol* 1999, 91, 128.
- Degamber, B.; Fernando, G. F. *MRS Bull* 2002, 27, 370.
- Crosby, P. A.; Powell, G. R.; Fernando, G. F.; France, C. M.; Waters, D. N.; Spooner, R. C. *Proceedings of the 7th Institute of Physics Conference on Sensors and Their Applications*; Augousti, A. T., Ed.; Dublin, Ireland; Institute of Physics: Surrey, UK, Sept 10–13, 1995.
- Marand, E.; Baker, K. R.; Graybeal, J. D. *Macromolecules* 1992, 25, 2243.
- Crosby, P. A.; Doyle, C. T.; Tuck, C.; Singh, M.; Fernando, G. F. *International Symposium on Smart Structures and Materials*; SPIE Series 3670; Claus, R. O.; Spillman Jr., W. B., Eds.; The Intl. Soc. for Optical Engineering: Newport Beach, CA, 1999; p 144.
- Degamber, B.; Dumitrescu, O. R.; Doyle, C. T.; Fernando, G. F. *Proceedings of the FRC Conference*; Gibson, A. G., Ed.; Conference Design Consultants: Newcastle upon Tyne, England, March 26–28, 2002.
- Stelleman, C. M.; Jeffrey, F. A.; Myrick, M. L. *Appl Spectrosc* 1995, 49, 392.
- Liu, T.; Martin, A.; Badcock, R.; Ralph, B.; Fernando, G. F. *Smart Mater Struct* 1997, 6, 464.
- Mijovic, J.; Andjelic, S.; Kenny, J. M. *Polym Adv Technol* 1996, 7, 1.
- Rogers, D. G.; Marand, E.; Hill, D. J. T.; George, G. A. *High Perform Polym* 1999, 11, 27.